

Науки о Земле Earth sciences

УДК 550.389.1

<https://doi.org/10.21440/2307-2091-2019-2-7-19>

Magnetic data interpretation to determine the depth of basement rocks and structural elements of Mandisha village, El-Bahariya Oasis, Western Desert, Egypt

Wael Ragab GAWESH^{1, 2, *},
Hossam Hassan MARZOUK²,
Aleksey Vladimirovich PETROV¹,
Igor⁷ Alekseevich MARAEV¹

¹Russian State Geological Prospecting University, Moscow, Russia

²National Research Institute of Astronomy and Geophysics (NRIAG), Cairo, Egypt

Relevance. The study area is located at Mandisha village, El-Bahariya Oasis, Western Desert, Egypt. It is suffering from lack of surface water. So it's important to search for another source of water (as groundwater) that important for everything for live. Based on the literature studies; the main aquifer in the study area is located in the Nubian sandstone aquifer, which located directly on the upper surface of the basement rocks. So the depth of the lower surface of the Nubian sandstone aquifer is equal to the depth of the upper surface of the basement rocks in the study area.

Objectives of the study. This study is used the analysis and interpretation of magnetic data to determine the depth of the basement rocks and the structural elements that affected on the basement rocks at Mandisha area in El-Bahariya Oasis, Western Desert, Egypt.

Research methodology. The Magnetic methods were applied to achieve these goals. One hundred and seventy four magnetic stations were acquired by Overhauser magnetometer instrument (GSM-19 "V7.0"). The magnetic data were processed by using Geosoft Oasis Montaj program. 2D Magnetic Profiles and 3D Magnetic Modeling were established to construct basement relief map in the study area. First Vertical Derivative Technique, Source Edge Detection Method and 3D Euler Deconvolution method were established to determine the locations and directions of faults that affected on the Basement Rocks in the study area.

Work results. The most important results of this study: 1. The depth of the basement rocks in the study area ranges from 1200 m to 2000 m. 2. The northeastern, northwestern and western parts of the study area are characterized by shallow depth of the basement rocks, while the southern and eastern parts of the study area are characterized by deep depth of the basement rocks. 3. Deep faults (more than 2000 m) were located at northern part of the study area. 4. The main direction faults in the study area are NE-SW and E-W direction.

Keywords: Magnetic Data Interpretation, 3D Euler Deconvolution, 2D Magnetic Profile, 3D Magnetic Modeling, Basement Rocks, faults, Geosoft, El-Bahariya Oasis, Western Desert, Egypt.

Introduction

The study area is located at Mandisha village in El-Bahariya Oasis, Western Desert, Egypt. It is located between latitudes 28° 16' 22'' N–28° 19' 14'' N and longitudes 28° 55' 40'' E–28° 59' 50'' E with an area of 36.13 km² (Fig. 1).

The study area is suffering from lack of surface water. So it's important to search for another source of water that important for living and everything for live as groundwater. Based on the literature studies; the main aquifer in the study area is located in the Nubian sandstone aquifer (Cenomanian age), which located directly on the upper surface of the basement rocks [1]. So the depth of the lower surface of the Nubian sandstone aquifer is equal to the depth of the upper surface of the basement rocks in the study area.

The analysis and interpretation of magnetic data were used for mapping the relief of the basement rocks in the study area. So, the main purpose of this study is to analyze and interpret the magnetic data for determining the depth of basement rocks in the study area and the structural elements (Faults and/or cracks) that affected the study area.


Our pattern recognitions criteria are based on the interpretation of magnetic data that applied on the total intensity magnetic map reduced to the pole (RTP Map). The interpretation of magnetic data includes five techniques which applied by Geosoft program: these techniques including First Vertical Derivative Technique, Source Edge Detection Method, 3D Euler Deconvolution, 2D Magnetic Profiling and 3D Magnetic Modeling. After that; the Magnetic interpretations have been compared with each other to determine the location of faults with high resolution.

Geology of the study area

The geology of the study area was described from the geological map of El-Bahariya Oasis and the stratigraphic succession of well No. 1 (Box-1) that located at El-Bahariya Oasis. These geological study includes surface and subsurface geology of the study area.

a) **The surface Geology of the study area** has been described from the geological map of Egypt, Sheet No. (NH 35 SE BAHARIYA) with a scale of 1 : 500 000 [2]. It was built by the Egyptian General petroleum Corporation in 1986 (Fig. 2). Surface Geology of the study area refers to the upper Cretaceous "Cenomanian age" and Quaternary age: 1. Upper Cretaceous deposits were represented by Bahariya Formation (Early Cenomanian age). It has deposited at widespread of the study area. Bahariya Formation consists of fine to coarse Ferruginous Sandstone intercalated with Shale. 2. Quaternary deposits were represented by

* wael_ragab2007@yahoo.com

 <http://orcid.org/0000-0002-5971-4839>

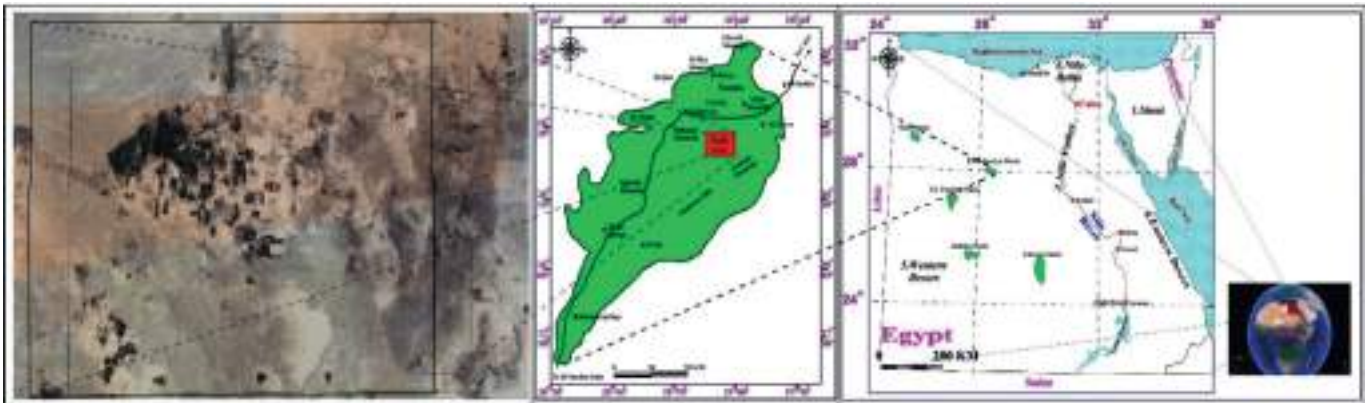


Figure 1. Location map of the study area.
Рисунок 1. Обзорная карта района работ.

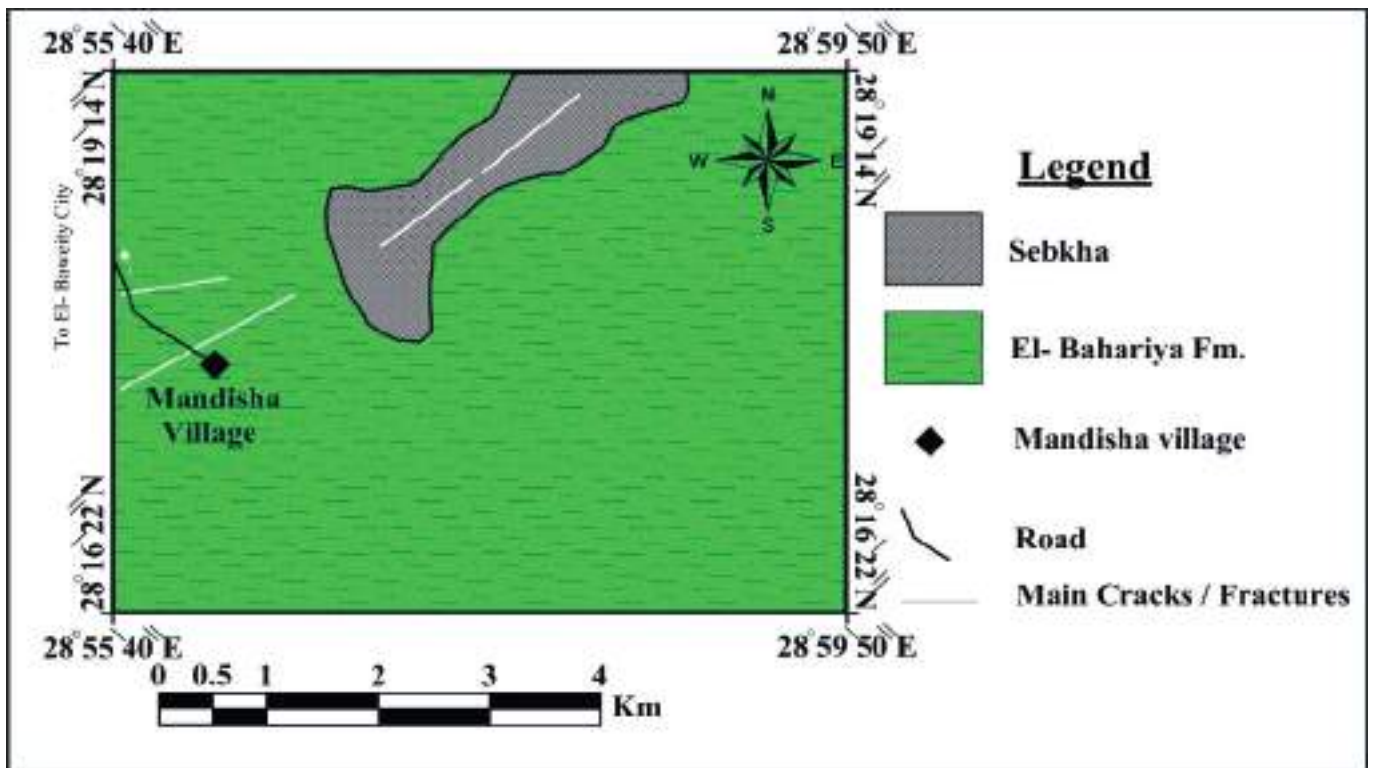


Figure 2. Geologic map of the study area [2].
Рисунок 2. Геологическая карта изучаемого района [2].

Sabkha deposits (which composed of Shale, Clay and Evaporate deposits). Sabkha deposits are concentrated at North Central part of the study area. 3. Structural elements which presented in the study area as cracks and/or fractures. The main direction of these fractures is NE–SW direction.

b) **Subsurface stratigraphy of El-Bahariya Oasis** were collected from well No. 1 (Box-1) that located at El-Bahariya Oasis with latitude $28^{\circ} 19' 27.5''$ N and longitude $28^{\circ} 58' 00''$ E with an Elevation 122 M (after [1, 3, 4]). A Brief description of the subsurface stratigraphic section of El-Bahariya Oasis from top to bottom layer is shown in (Table 1 and Fig. 3).

Methodology

In this study, the magnetic data were analyzed and interpreted for determining the depth of the basement rocks and the structural elements that affected on the basement rocks of the study area.

1. Magnetic data acquisition

One hundred and seventy four magnetic stations were measured to cover the study area (Fig. 4, a). Magnetic data were carried out using one Overhauser magnetometers for both field survey and base station recordings. The model of Overhauser magnetometer, which used for magnetic acquisition, is ((GSM-19) V7.0), made in Canada (since 1980), with sensitivity 0.022 nT (Fig. 4, b and Fig. 4, c) [5]. Magnetic stations were measured in the study area every 300–500 m. The base station was recorded every 3–5 hours during field measurements. It was located at the Eastern part of the study area with longitude $28^{\circ}59'30.99''$ E and latitude $28^{\circ}17'57.4''$ N with an absolute value of 42592.5γ.

Table 1. Composite stratigraphic section of El-Bahariya Oasis (after [1, 3, 4]).

Таблица 1. Стратиграфический разрез оазиса Эль-Бахария (по данным [1, 3, 4]).

Formation name	Age	Lithology	Thickness, m	Note
Olivin Basalt	Early Miocene	The olivine basalt consists of basalt flows and sills	20	Neogene rocks are represented by volcanic rocks "Olivine Basalt"
Radwan Formation	Oligocene	Radwan Formation consists of dark brown Ferruginous Sandstone	35	Olivine Basalt lies on Radwan formation
Hamra Formation	Middle & Late Eocene	Hamra Formation is composed of Limestone intercalated with clastic rocks, forming reef-like structures with dips of 10–40°	60	Radwan Formation lies on Hamra formation
Qazzun Formation	Middle Eocene	Qazzun Formation consists of white Limestone intercalated with hard Dolomitic Limestone	32	Hamra Formation lies on Qazzun Formation
Naqb Formation	Early-Middle Eocene	Naqb Formation consists of chalk intercalated with Dolomitic Limestone	67	Qazzun Formation lies on Naqb Formation
<i>Disconformity because the absence of Paleocene Sediments</i>				
Khoman Chalk Formation	Maastrichtian	Khoman Chalk Formation consists of Chalk and limestone with hard dolomitic limestone at the top	42	Naqb Formation lies on Khoman Chalk Formation
El-Hefhuf Formation	Turonian-Santonian	El-Hefhuf Formation consists of carbonate rocks intercalated with Dolostone rocks	43	Khoman Chalk Formation lies on El-Hefhuf Formation
El-Heiz Formation	Late Cenomanian	El-Heiz Formation is composed of carbonate rocks intercalated with Dolostone rocks	30	El-Hefhuf Formation lies on El-Heiz Formation
El-Bahariya Formation	Cenomanian	El-Bahariya Formation consists of Sandstone intercalated with Shale. El-Bahariya Formation consists of 4 zones. Zone A = 215 m, Zone B = 92 m, Zone C = 220 m and Zone D = 175 m	702	El-Heiz Formation lies on El-Bahariya Formation
<i>Disconformity because the absence of Ordovician, Silurian, Devonian, Carboniferous, Permian, Triassic and Jurassic Sediments</i>				
Cambrian rocks	Cambrian	Cambrian rocks, composed of dense granite, with a depth of Basement rocks 1822 m	–	–

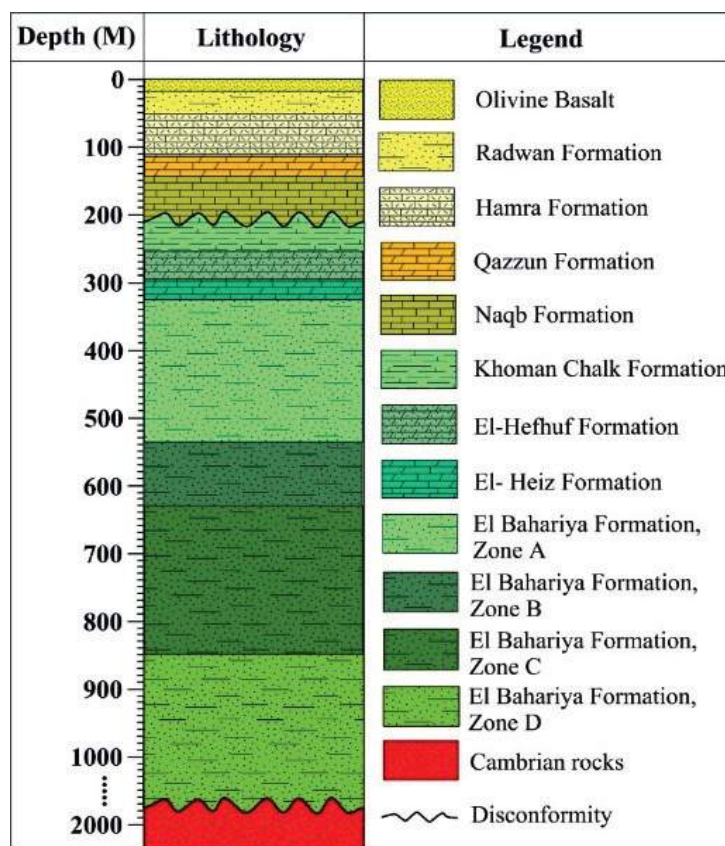


Figure 3. Composite stratigraphic column of El-Bahariya Oasis, Western Desert, Egypt (after [3, 4]).

Рисунок 3. Стратиграфический разрез оазиса Эль-Бахария, Западная пустыня, Египет (по данным [3, 4]).

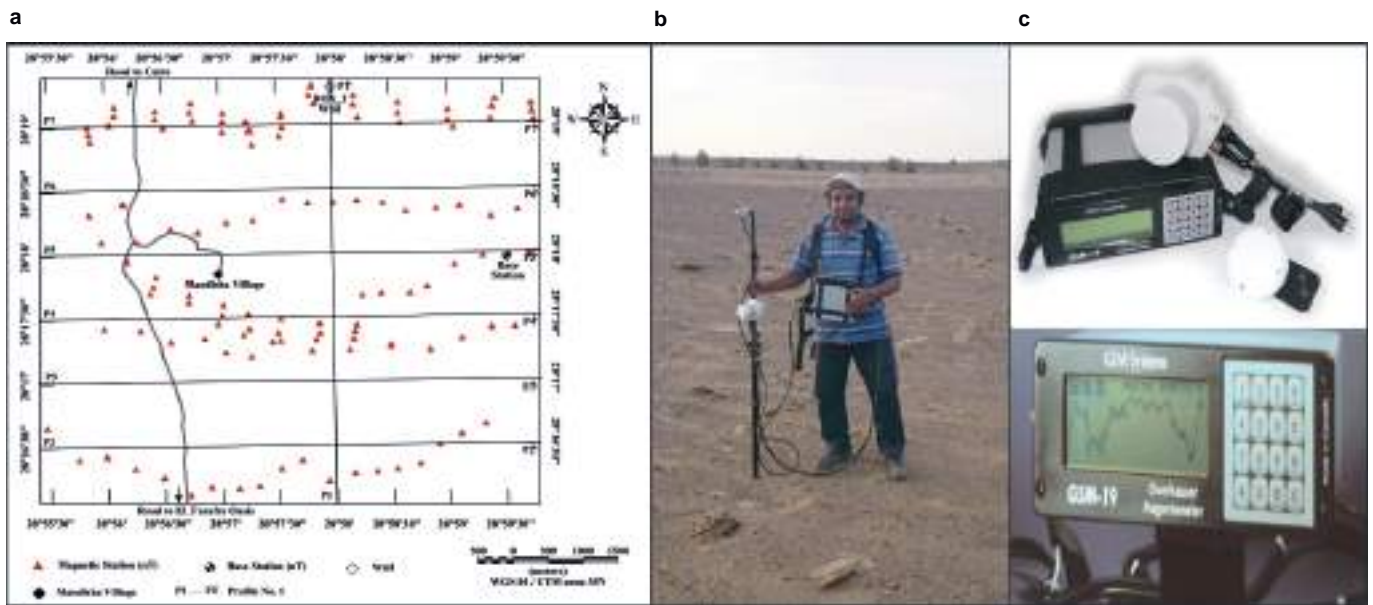


Figure 4. Magnetic Data Acquisition. a – location Map of Magnetic Stations, base station and magnetic profiles in the study area; b – when measuring magnetic data in the study area; c – Overhauser magnetometer system (GSM-19 v7.0).

Рисунок 4. Получение магниторазведочных данных. а – обзорная карта магнитных пунктов, опорных пунктов и магниторазведочных профилей в районе проведения исследований; б – процесс получения данных магниторазведки в районе проведения исследований; в – магнитометр с датчиком Оверхаузера (GSM-19 v7.0).

Table 2. Examples of magnetic data that exported from an Overhauser magnetometer to the computer – in file format: XYZ format (linear oriented).

Таблица 2. Примеры данных магниторазведки, импортированных с магнитометра на компьютер, – в формате XYZ (прямолинейные).

/ Gem Systems GSM-19GW 0103903 v7.0 15 11 2011 M ew5fpl.v7s										
/ ID 0 file 01survey.m 23 11 96										
/										
/	X	Y	Elevation	nT	sq	cor-nT	Sat	Time	Picket-X	Picket-Y
Line 000020										
	028.2996220	028.9952480	000150	42594.40	99	000000.00	07	045644.0	0.00	0.00
	028.2996216	028.9952480	000150	42594.39	99	000000.00	07	045650.0	0.00	0.00
	028.2996421	028.9952438	000150	42595.68	99	000000.00	07	045659.0	0.00	0.00
	028.2996416	028.9952438	000150	42595.76	99	000000.00	07	045705.0	0.00	0.00
	028.2996472	028.9952860	000152	42594.48	99	000000.00	07	045717.0	0.00	0.00
	028.2996463	028.9952848	000152	42594.46	99	000000.00	07	045723.0	0.00	0.00
	028.2996054	028.9952498	000152	42594.09	99	000000.00	07	045738.0	0.00	0.00

Magnetic readings were stored in the memory of Overhauser magnetometer, after that; all data were loaded from Overhauser magnetometer to the computer (Table 2) for preparing magnetic data for necessary corrections and interpretations.

2. Magnetic data processing

Magnetic data were corrected for daily variations correction before starting the interpretation. Daily variations in the Earth's magnetic field sometimes had an amplitude more than 10 gammas (which caused by sunspots). Therefore, the base station was used for magnetic correction. The daily variations of the geomagnetic field were subtracted from the Magnetic field data. The corrected magnetic values were contoured by Geosoft program with contour interval 2 nT [6] and represented by the total intensity magnetic map (Fig. 5, a).

Total Intensity Magnetic Map (TIM Map). TIM Map is a reflection of lateral changes in the magnetic properties of the Basement Rocks in the study area (Fig. 5, a). Thus, the magnetic expression of various structural features depends on the existence and magnitude of their magnetic contrasts. The qualitative interpretation of the Total Intensity Magnetic Map begins with a visual inspection of the forms and directions of the main magnetic anomalies. TIM Map has magnetic anomaly values between 42 500 nT and 42 620 nT. The high magnetic anomalies indicate that the depth of basement rocks is shallow depth, so the thickness of sedimentary cover is thin. The high magnetic anomalies are represented at Northeastern part of the study area. On the other side, the low magnetic anomalies indicate on a deep basement rocks (thick sedimentary cover). The low magnetic anomalies are located at the Southeastern part of the study area. Generally, the magnetic anomaly increases from Southeastern part to Northeastern part of the study area, which indicate that the depth of basement rocks increase from Northeastern part to Southeastern part of the study area.

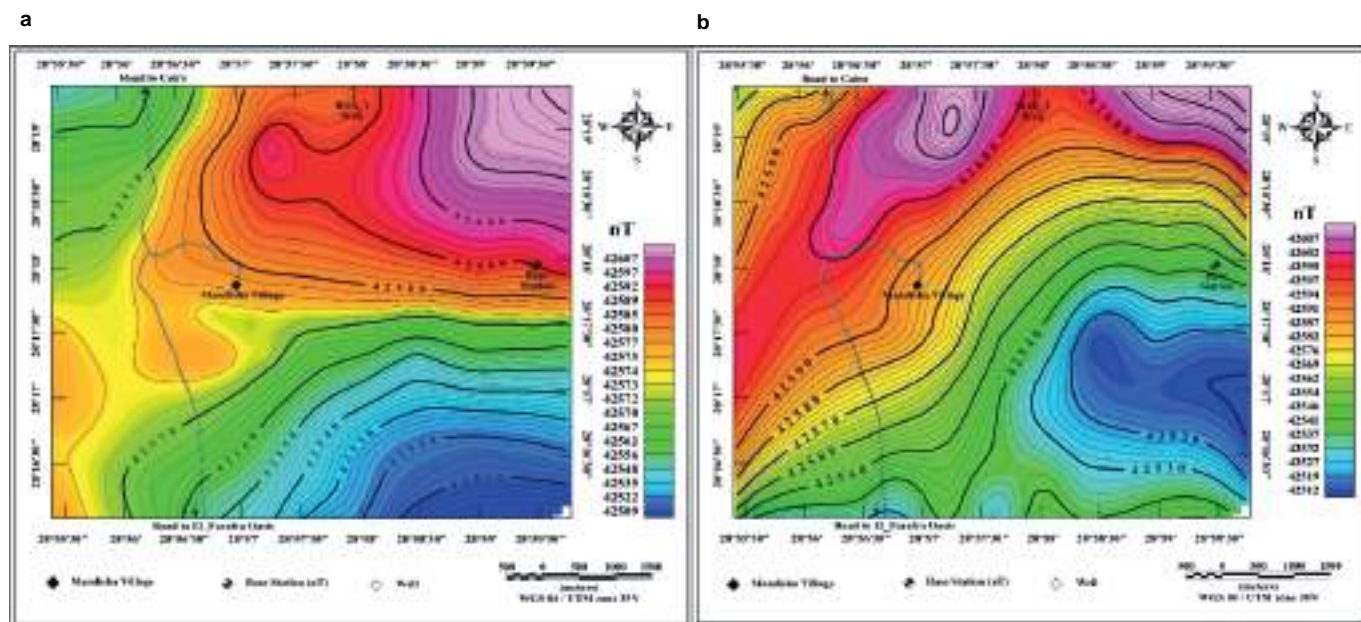


Figure 5. Magnetic Data Processing. a – Total Intensity Magnetic Map (TIM Map); b – the Total Intensity Magnetic Map Reduced To the Pole (RTP Map).

Рисунок 5. Обработка данных магниторазведки. а – магнитная карта суммарной интенсивности (TIMMap); б – магнитная карта суммарной интенсивности, приведенной к полюсу (RTPMap).

The Total Intensity Magnetic Map Reduced to the Pole (RTP Map). The total intensity magnetic data were reduced to the magnetic pole (Fig. 5, b) to overcome the distortion in anomaly appearance. This appearance depends on the magnetic latitude of the survey area and depends on the dip angle of the magnetization vector in the body using magnetic parameters such as inclination angle (41.2177°), declination angle (3.9282°), magnetic field strength (42488.2 nT) and the height of device’s sensor from earth surface (1 m). This mathematical procedure was first described by [7–11].

A general outlook to the magnetic map reduced to the magnetic pole (Fig. 5, b) in comparison with the total magnetic intensity map (Fig. 5, a) reflects the northward shift in the positions of the inherited magnetic anomalies due to elimination of inclination of magnetic field at this area. The RTP map exhibits different magnetic anomalies while ranging from 42 512 nT to 42 607 nT. The northeastern and northwestern parts of the study area reveal high magnetic anomalies where the eastern, southern, and southeastern parts exhibit low magnetic anomalies.

3. Magnetic data interpretations

Interpretation of magnetic data includes five Techniques which applied by Geosoft program to determine the structural elements (Faults) and the depths of the upper surface of the basement rocks that caused the magnetic anomalies in the study area. These techniques include (First Vertical Derivative Technique, Source Edge Detection Method, 3D Euler Deconvolution, 2D Magnetic Profiles and 3D Magnetic Modeling).

a) **First Vertical Derivative Technique (FVD Technique).** Many authors were calculated First Vertical Derivative of potential data (Gravity and/or Magnetic data) as [12–17 and others].

The working equation of Rosenbach [17], equation (1):

$$\frac{\partial^2 g}{\partial z^2} = \frac{1}{24} \left(96g(0) - 18 \sum_{i=1}^4 gi(S) - 8 \sum_{i=1}^4 gi(s\sqrt{2}) + \sum_{i=1}^8 gi(s\sqrt{5}) \right), \tag{1}$$

where $\frac{\partial^2 g}{\partial z^2}$ is the first vertical derivative of gravity or magnetic potential field. S is the grid spacing. g(0) is the gravity or magnetic value at the point of calculation; $\sum_{i=1}^4 gi(S) - 8, \sum_{i=1}^4 gi(s\sqrt{2}), \sum_{i=1}^8 gi(s\sqrt{5})$ are summation of gravity or magnetic data values at the 4, 4 and 8 points lying on the three concentric circles of radials, $(s\sqrt{2})$ and $(s\sqrt{5})$ respectively.

FVD Technique acts as a filter. FVD Technique emphasizes the expression of local features of magnetic anomalies and eliminates the effect of regional anomalies. The first vertical derivative map was applied on RTP Map. In FVD Map (Fig. 6), zero contour lines show the contact lines between highly polarized sources (which indicate that the depth of basement rocks are shallow) and less polarized sources (which indicate that the depth of basement rocks are deep) at the same level of measurement. These Zero contour lines indicate on the faults that affected on the basement rocks in the study area. The main directions of these faults are N–S, NE–SW and NW–SE directions. Negative magnetic values show deep basement rocks, which located at the Eastern and Northwestern parts of the study area. Where, the positive magnetic values show shallow basement rocks, which located at north-eastern and western parts of the study area.

b) **Source Edge Detection Method (SED Method).** The source edge detection (SED) system is used to locate the approximate edges and down-gradient directions of source bodies from magnetic or gravity gridded data sets [18]. Blakely and Simpson were

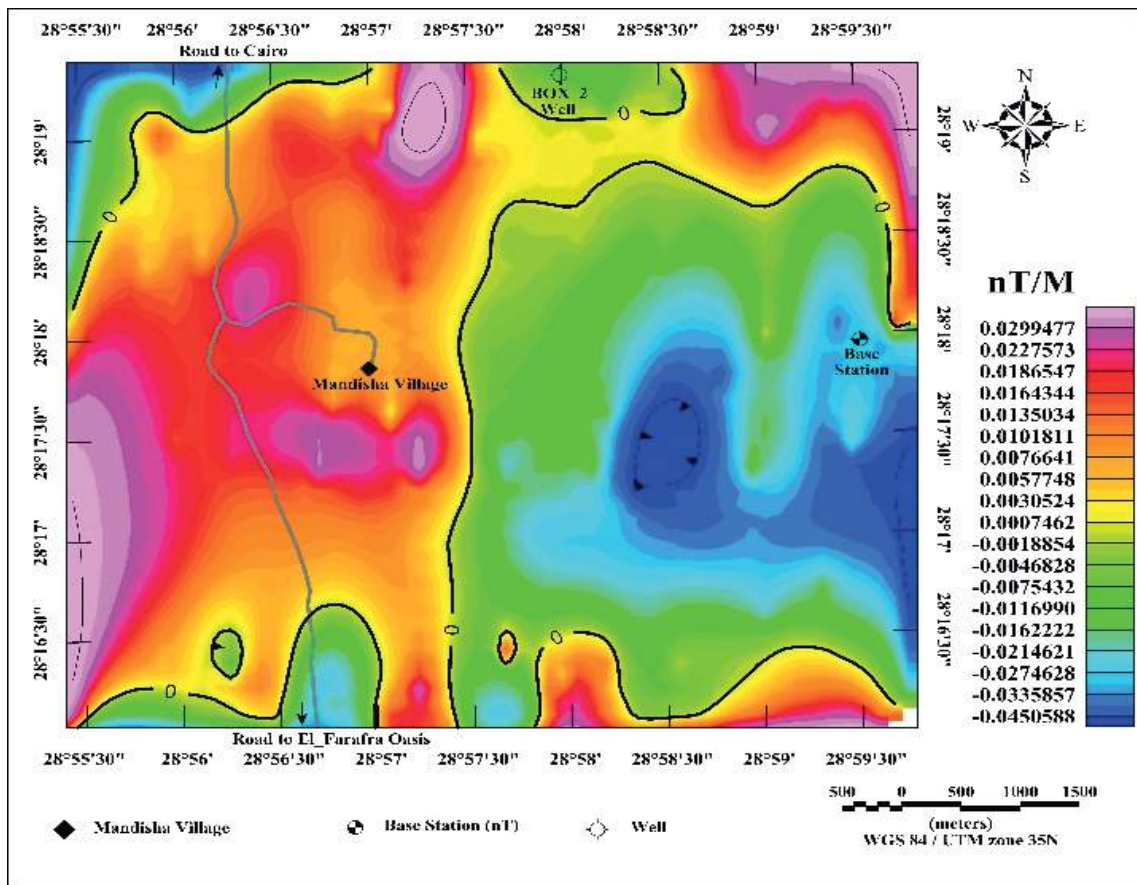


Figure 6. First Vertical Derivative Map (FVD Map).
Рисунок 6. Карта первых производных (FVD Map).

used SED Method to calculate reduction to the pole grid and total horizontal derivative grid from the total magnetic field grid [18]. The Geosoft program was used to calculate RTP Grid and its horizontal gradient. Two maps were created by applying SED Method: First map is horizontal gradient Map of RTP Grid, which containing on oval-shaped magnetic anomalies and their axes indicate on the direction of faults that appeared in the study area (Fig. 7, a). Second Map is geological contacts Map (faults) that detected on RTP Map. This map shows the locations and directions of faults in the study area. The main directions of faults are NE-SW and E-W directions (Fig. 7, b).

c) **3D Euler Deconvolution.** Recently, 3D Euler Deconvolution method has been widely used in the automatic interpretation of Magnetic and Gravity data. It has emerged as a powerful tool for direct determination of depth of the gravity and magnetic bodies. Also, it uses for determination the dykes and contacts with remarkable accuracy [19–24].

Usually the locations and depths of any sources (x_0, y_0, z_0) can be determined by using the following equation (2):

$$\frac{\partial f}{\partial x}(x-x_0) + \frac{\partial f}{\partial y}(y-y_0) + \frac{\partial f}{\partial z}(z-z_0) = SI(B-f), \tag{2}$$

where f is the observed field at location (x, y, z) and B is the base level of the field [regional value at the point (x, y, z)] and SI is the structural index or degree of homogeneity [19]. The equation (2) is solved for the source position by least-squares inversion of a moving window of data points. To obtain an accurate estimation of the source location, the field data used must adequately sample the anomalies present in the data.

In the present study, the 3D Euler Deconvolution technique was applied to determine the locations and depths of the faults in the study area. The obtained solutions of the interpretations of 3D Euler Deconvolution of magnetic data are shown in Fig. 8. Euler solutions were applied on RTP Grid by structural indexes 0, 1, 2, and 3 to select the best solution. Structural index zero “ $SI = 0$ ” indicates on Contact/Step (Fig. 8, a), structural index one “ $SI = 1$ ” indicates on Sill/Dyke (Fig. 8, b), structural index two “ $SI = 2$ ” indicates on Cylinder/Pipe (Fig. 8, c) and structural index three “ $SI = 3$ ” indicates on Sphere/Barrel/Ordnance (Fig. 8, d) [6]. The structural index $SI = 0$ gives better solutions than the structural indices 1, 2 and 3, because the data is concentrated in the study area (Fig. 8, a).

d) **2D Magnetic Profiles.** 2D magnetic profiles were applied by GM-SYS program on RTP Map [25]. GM-SYS program provide an easy interface for creating and managing models to fit observed magnetic data.

GM-SYS program was used to estimate the depth of the upper surface of the basement rocks using the following parameters: **1. International Geomagnetic Reference Field (IGRF)** for a point in the study area (which located at longitude $28^{\circ}57'29.988''E$, latitude $28^{\circ}18'00''N$ with Elevation 134 M, time of measurement 09.10.2015) to obtain the Total Magnetic Field = 42488.2 nT, Inclination Angle = 41.2177° and Declination Angle = 3.9282° . **2. The used Parameters for the sedimentary layer** (almost

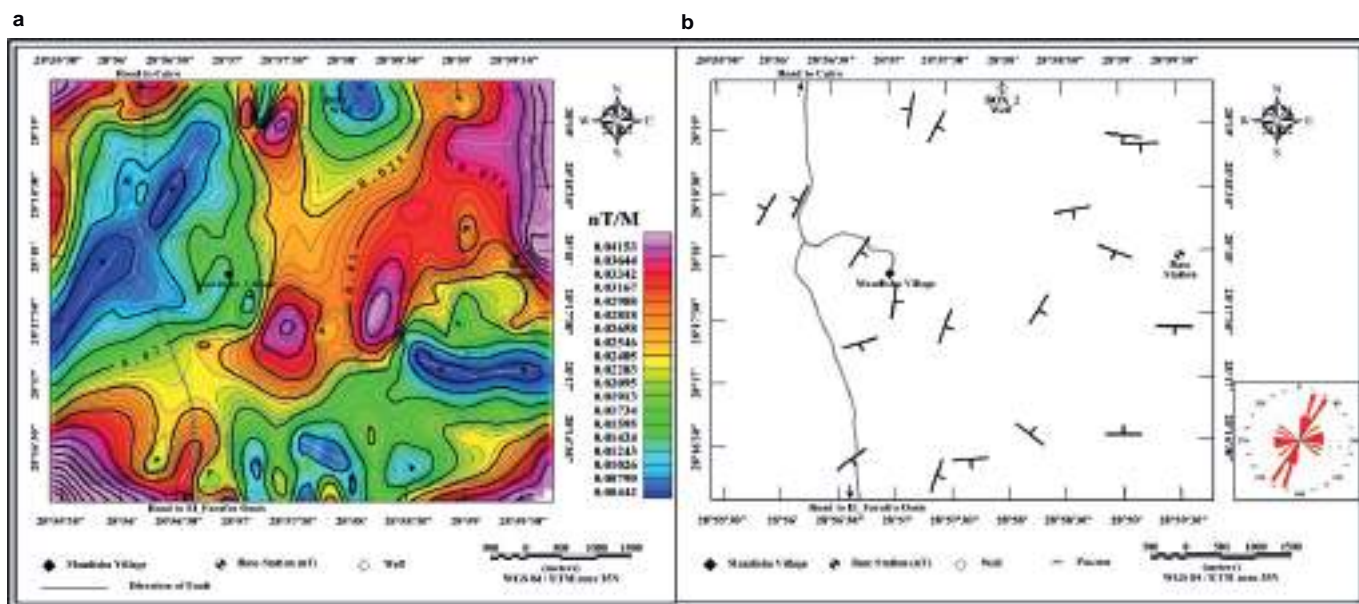


Figure 7. Source Edge Detection Method. a – horizontal gradient Map of RTP Grid; b – geological contacts Map (faults).
 Рисунок 7. Метод определения границ источника. а – карта горизонтального градиента RTP; б – карта геологического контакта (разломы).

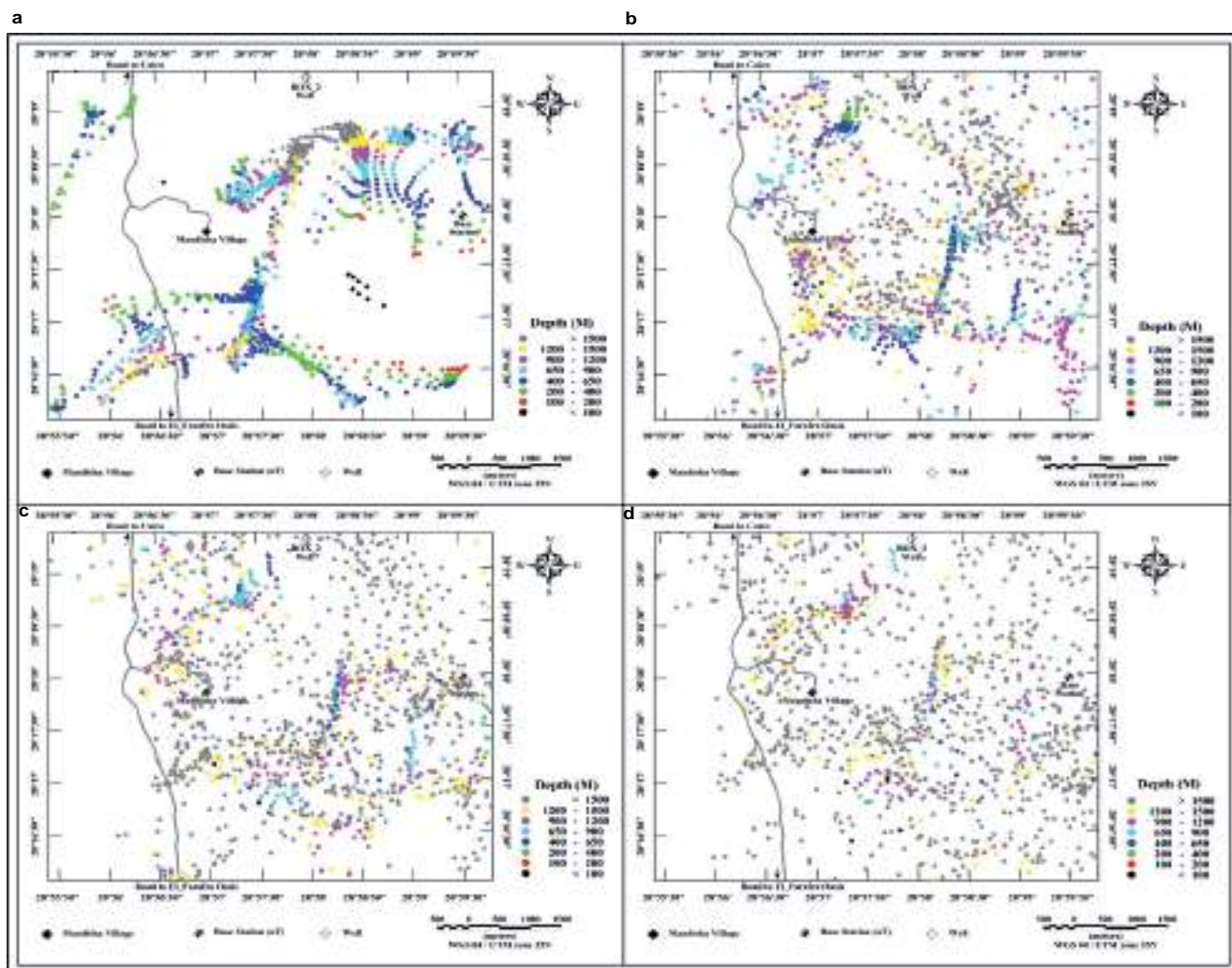


Figure 8. 3D Euler Deconvolution method. a – Euler Solutions of Structural Index = 0; b – Euler Solutions of Structural Index = 1; c – Euler Solutions of Structural Index = 2; d – Euler Solutions of Structural Index = 3.

Рисунок 8. 3D метод деконволюции Эйлера. а – решения уравнений Эйлера структурного индекса = 0; б – решения уравнений Эйлера структурного индекса = 1; в – решения уравнений Эйлера структурного индекса = 2; г – решения уравнений Эйлера структурного индекса = 3.

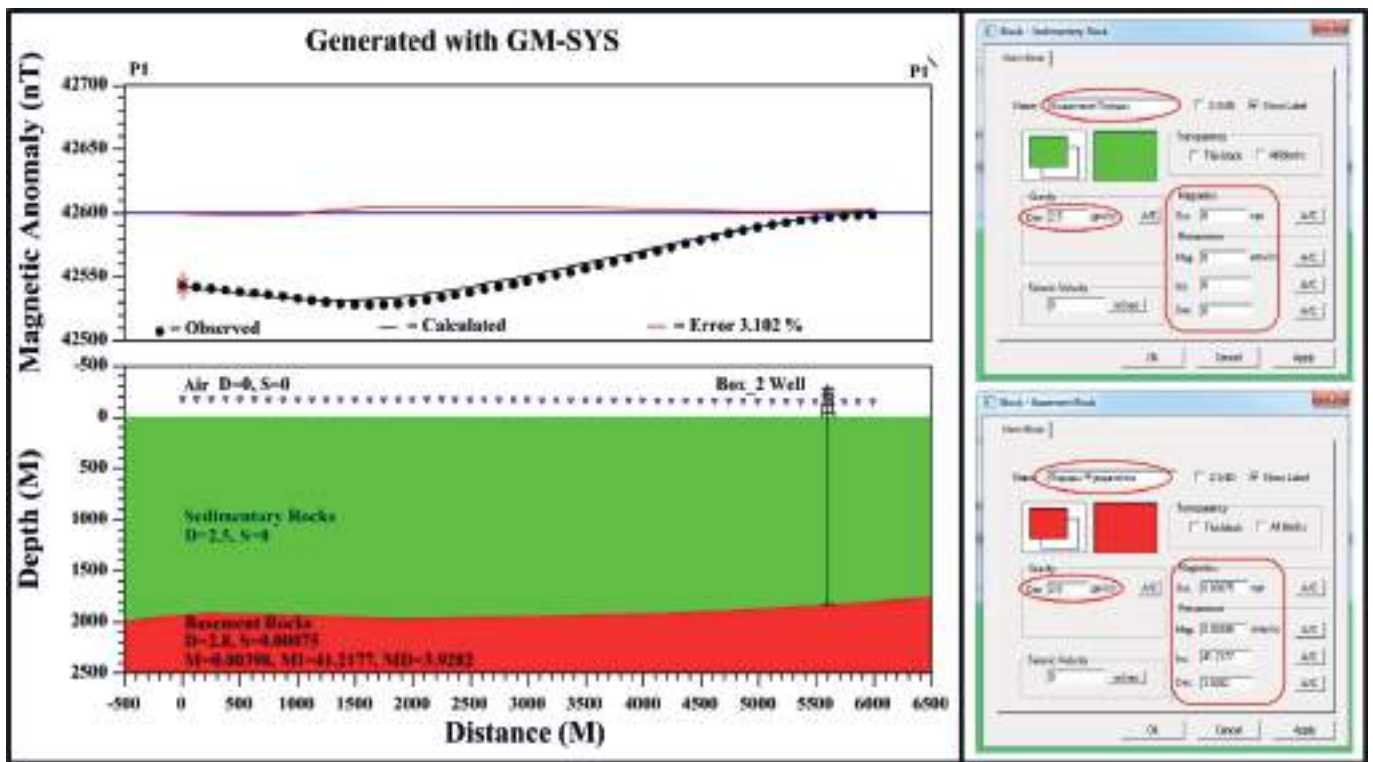


Figure 9. 2D Magnetic profile “P1” and used parameters in GM-SYS program for the sedimentary layer and Basement layer.

Рисунок 9. 2D магниторазведочный профиль P1 и применяемые параметры в программе GM-SYS для слоя осадочных пород и слоя подстилающих пород.

Sandstone intercalated with Shale, Clay and Limestone): the average Density of the Sedimentary Layer is 2.5 gram/cm³, Magnetic Susceptibility = 0 CGS, Remanence Magnetization = 0 emu/cm³, Remanence Inclination = 0° and Remanence Declination = 0° (Fig. 9). **3. The used parameters for the Basement layer** (almost Granite): the average Density of the Basement layer is 2.8 gram/cm³, Magnetic Susceptibility = 0.00075 CGS, Remanence Magnetization = 0.00398 emu/cm³, Remanence Inclination = 41.2177° and Remanence Declination = 3.9282° (Fig. 9).

Seven magnetic profiles were applied on RTP Map (Fig. 4, a). The first profile (P1) passes through well (BOX_2) with direction from South to North and other profiles (P2, P3, P4, P5, P6 and P7) were oriented from West to East. Profile “P1–P1” is perpendicular on other profiles; it has a direction from South to North with a length of 6130 M. This profile passes through the borehole (Box_2), which is located at 28° 19' 27.5" N and 28° 58' 00" E with depth of Basement rocks 1822 M. The depth of Basement Rocks along profile P1–P1 varies from 1822 m to 1963 m (Fig. 9).

The other profiles (P2, P3, P4, P5, P6 and P7) were oriented from West to East. The second Profile “P2–P2” has a length 7187 M. Profile P2 passes through Profile P1 with depth of Basement 1929 M. The depth of Basement Rocks along Profile P2 ranges from 1820 m to 1998 m (Fig. 10, a). The third Profile “P3–P3” has a length 7161 M. Profile P3 passes through profile P1 with depth of Basement 1960 M. The depth of Basement Rocks along Profile P3 ranges from 1630 m to 2150 m (Fig. 10, b). The fourth Profile “P4–P4” has a length 7174 M. Profile P4 passes through Profile P1 with depth of Basement 1847 M. The depth of Basement Rocks along Profile P4 ranges from 1580 m to 1996 m (Fig. 10, c). The fifth Profile “P5–P5” has a length 7161 M. Profile P5 passes through profile P1 with depth of Basement 1957 M. The depth of Basement Rocks along Profile P5 ranges from 1714 m to 2065 m (Fig. 10, d). The sixth Profile “P6–P6” has a length 7161 M. Profile P6 passes through profile P1 with depth of Basement 1701 M. The depth of Basement Rocks along Profile P6 ranges from 1588 m to 1742 m (Fig. 10, e). The seventh Profile “P7–P7” has a length 7174 M. Profile P7 passes through profile P1 with depth of Basement 1500 M. The depth of Basement Rocks along Profile P7 ranges from 1274 m to 1564 m (Fig. 10, f).

The results of 2D magnetic profiles were used to construct a depth map of the basement rocks in the study area by Geosoft program with contour interval 20 m (Fig. 11). The depth of the basement rocks in the study area is ranging from 1300 m to 2100 m. The northeastern, northwestern and western parts of the study area are characterized by shallow basement rocks, while the southern and eastern parts of the study area are characterized by deep basement rocks. Thus, the depth of basement rocks is increasing from northeastern, northwestern and western parts toward eastern part of the study area (Fig. 11).

e) **3D Magnetic Modeling.** 3D Magnetic modeling was carried out on RTP Grid by GMSYS-3D software. GMSYS-3D is a package for 3D modeling of gravitational and magnetic grids. The model is determined by number of surface layers, with its density, magnetic susceptibility and Remanence magnetization that distributed and defined for each layer [26].

The GMSYS-3D program is used to perform 3D magnetic modeling in order to obtain the relief of the basement rocks and relief of the earth's surface relatively to sea level using the following parameters: **1. The used parameters for Earth's surface layer** are: average Density 2.5 gram/cm³, Magnetic Susceptibility = 0 CGS, Remanence Magnetization = 0 emu/cm³, Remanence Inclination = 0° and Remanence Declination = 0° (Fig. 12, a). **2. The used parameters for Basement Layer** are: average density 2.8 gram/cm³, Magnetic Susceptibility = 0.00075 CGS, Remanence Magnetization = 0.00398 emu/cm³, Remanence Inclination = 41.2177° and Remanence Declination = 3.9282° (Fig. 12, c).

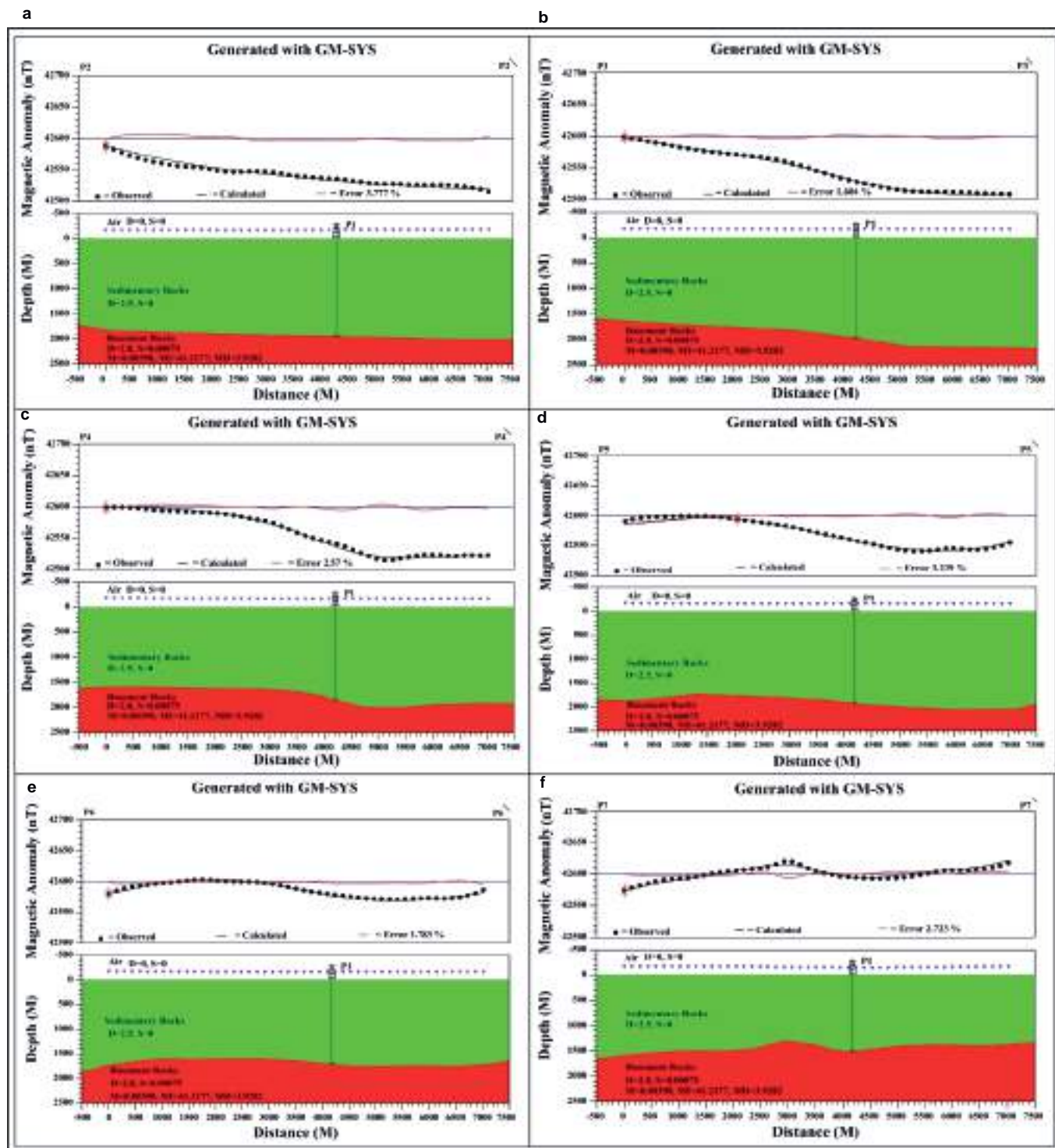


Figure 10. 2D Magnetic Profiles. a – 2D Magnetic Profile P2; b – 2D Magnetic Profile P3; c – 2D Magnetic Profile P4; d – 2D Magnetic Profile P5; e – 2D Magnetic Profile P6; f – 2D Magnetic Profile P7.

Рисунок 10. 2D магниторазведочные профили. а – 2D магниторазведочный профиль P2; б – 2D магниторазведочный профиль P3; в – 2D магниторазведочный профиль P4; г – 2D магниторазведочный профиль P5; д – 2D магниторазведочный профиль P6; е – 2D магниторазведочный профиль P7.

After applying 15 iterations by GMSYS-3D software, the results of 3D Magnetic Modeling shows that the thickness of the sedimentary layer in the study area is ranging from –1200 m to –2000 m. The thin thickness of the sedimentary layer is located at the northeastern, northern and western parts of the study area (the depth of the basement rocks is more than –1450 m). While the thick thickness of the sedimentary layer is located at the eastern part of the study area (the depth of the basement rocks is less than –1700 m) (Fig. 12, b).

Discussion

In this study, the depth of the basement rocks determined by 2D magnetic profiles and 3D magnetic modeling. The matching between the Basement Depth Map (Fig. 11) and 3D magnetic modeling (Fig. 12, b) is very high. The Basement Depth Map and

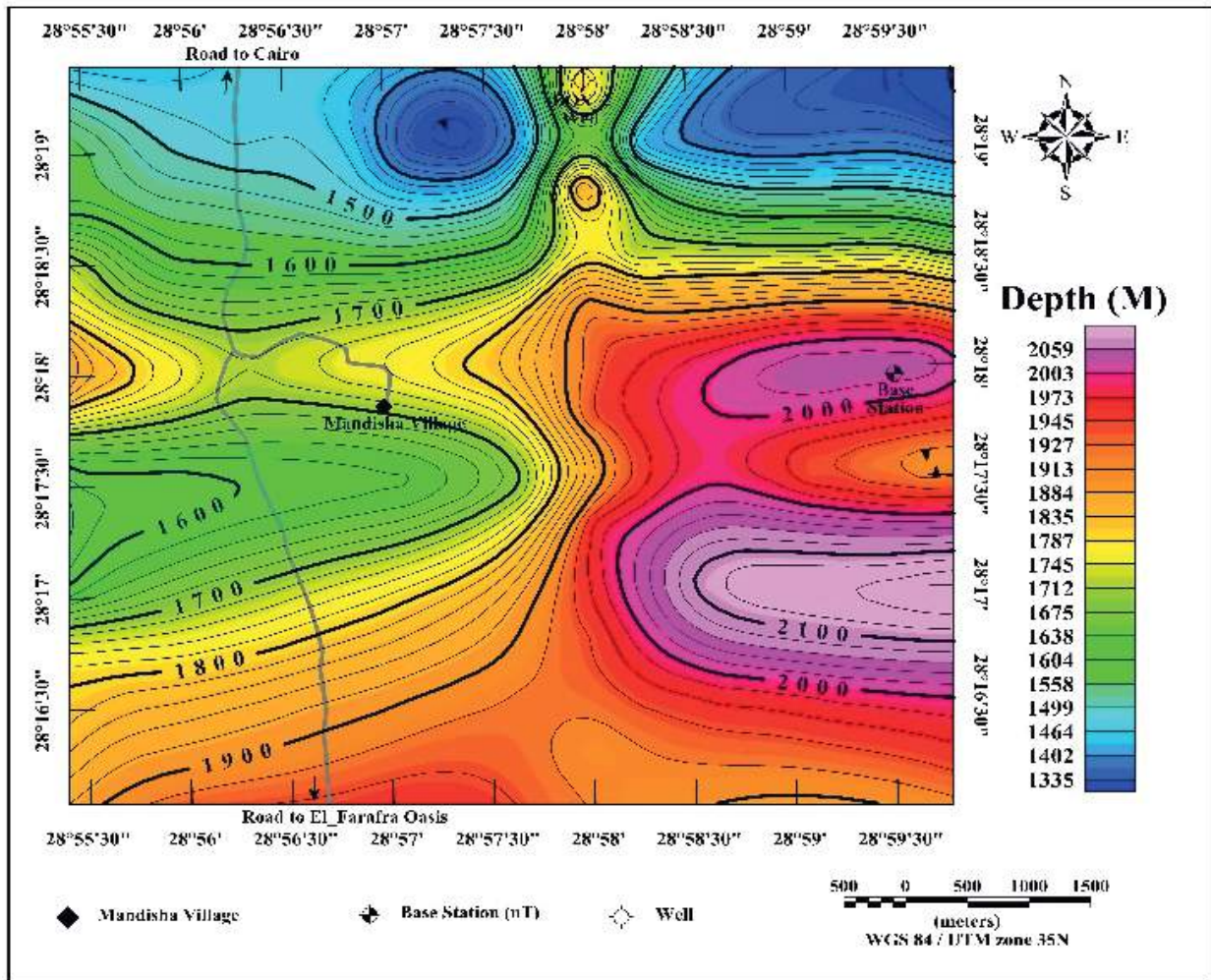


Figure 11. Basement Depth Map.
Рисунок 11. Карта глубины залегания фундамента.

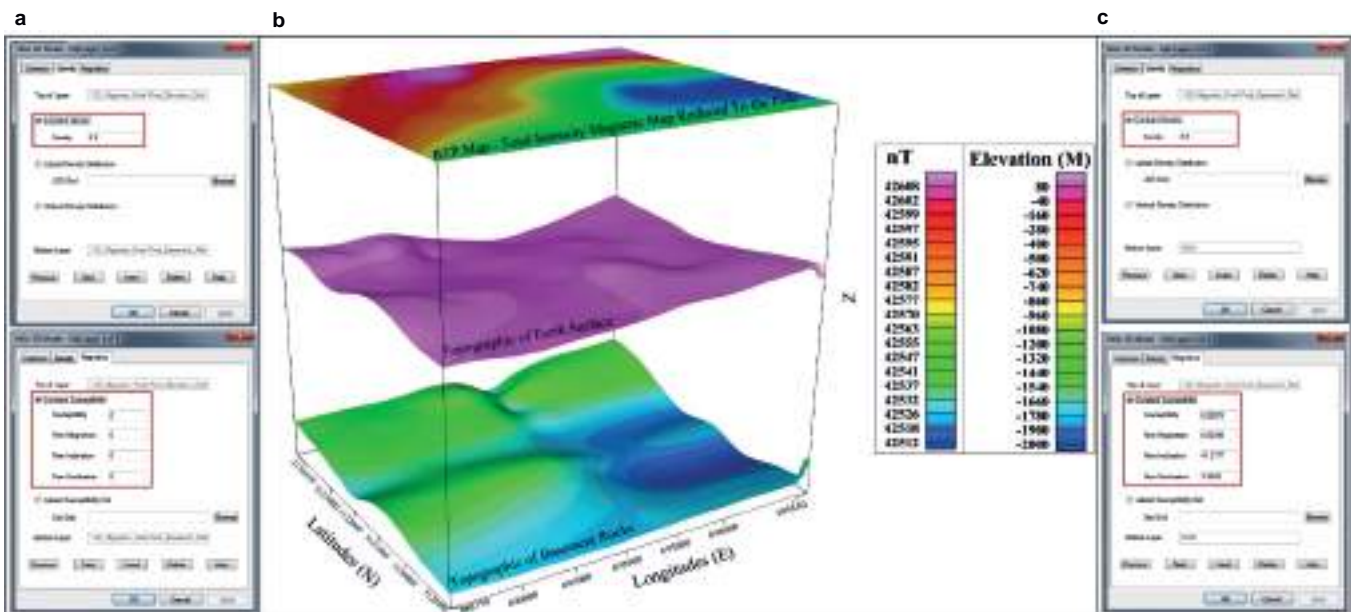


Figure 12. 3D Magnetic Modeling. a – used parameters in the GMSYS-3D program for the earth's surface Layer; b – 3D magnetic modeling, including Basement layer, Earth's surface layer and RTP Map; c – used parameters in the GMSYS-3D program for Basement layer.
Рисунок 12. 3D моделирование магниторазведочных задач. а – применяемые параметры в программе GMSYS-3D для слоя земной поверхности; б – 3D моделирование магниторазведочных задач, включая слой подстилающих пород, слой земной поверхности и магнитной карты суммарной интенсивности, приведенной к полюсу; в – применяемые параметры в программе GMSYS-3D для слоя подстилающих пород.

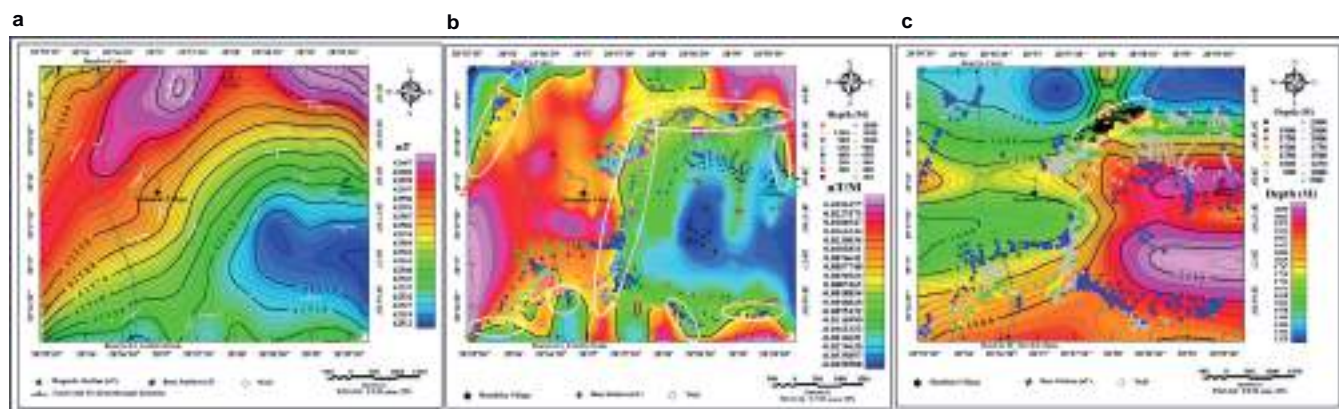


Figure 13. Integrations between the interpretation methods. a – integration between SED technique and RTP Map; b – integration between FVD method and 3D Euler Deconvolution with a structural index = 0; c – integration between 3D Euler Deconvolution with a structural index = 0 and Basement Depth Map.

Рисунок 13. Интеграции между методами интерпретации. а – интеграция между SED методом и магнитной картой RTP; б – интеграция между методом FVD и 3D методом деконволюции Эйлера со структурным индексом = 0; в – интеграция между 3D методом деконволюции Эйлера со структурным индексом = 0 и картой глубины залегания фундамента.

3D magnetic modeling shows that; the deep depth of the basement rocks are located at the eastern part, and many places in the southern part of the study area. But the shallow depth of the basement rocks are located at northeastern, northern and western parts of the study area.

The basement rocks in the study area were affected by many faults that determined by First Vertical Derivative technique (FVD), Source Edge Detection method (SED) and 3D Euler Deconvolution method. The integration between results of SED method and RTP Map shows that; the down-through of faults were directed to low values of magnetic anomalies of RTP map (Fig. 13, a). The Results of FVD method and 3D Euler Deconvolution with structural index (SI) = 0 determine the locations of faults in the study area (Fig. 13, b). Zero contour lines at FVD Map are show the contact lines between shallow and deep basement rocks at the same level of measurement. These Zero contour lines indicate on the locations of faults that affected on the basement rocks in the study area. 3D Euler Deconvolution with structural index (SI) = 0 also used to determine the locations and depths of these faults in the study area. The results show high matching between two methods. The main direction of these faults in the study area are NE–SW and E–W directions (Fig. 13, b).

The comparing between 3D Euler's Deconvolution with a structural index = 0 and Basement Depth Map is showing that; many faults are deep faults (their depth more than 2000 m) and reaching to the basement rocks. These deep faults were determined at northern part of the study area (Fig. 13, c).

Results

As mentioned in this research, the most important results of this study: **1.** The depth of the basement rocks in the study area ranges from 1200 m to 2000 m. **2.** The northeastern, northwestern and western parts of the study area are characterized by shallow depth of the basement rocks, while the southern and eastern parts of the study area are characterized by deep depth of the basement rocks. **3.** Many faults are deep (their depth more than 2000 m) and dissect the basement rocks, these faults located at northern part of the study area. **4.** The main direction faults in the study area are NE–SW and E–W direction.

REFERENCES

1. Moustafa A. R., Saoudi A., Moubasher A., Mohamed I., Molokhia H., Schwartz B. 2003, Structural setting and tectonic evolution of the Bahariya Depression, Western Desert, Egypt. *GeoArabia*, vol. 8, no. 1, pp. 91–124.
2. Egyptian Military Survey "EMS" Topographic Map of El-Bahariya Oasis. Scale 1:500000, Sheet No. NH 35 SE BAHARIYA, Western Desert, Egypt. 1986.
3. Diab M. S. 1972, Hydrogeological and Hydrochemical studies of the Nubian Sandstone water-bearing complex in some localities in United Arab Republic. PhD Thesis, Assiut University, Egypt.
4. Said R. 1962, The Geology of Egypt. Amsterdam, Netherlands, Elsevier, 377 p.
5. GEM GSM-19 Cost Effective and High Precision Overhauser Magnetometer. URL: <http://www.gemsys.ca/rugged-overhauser-magnetometer>
6. Geosoft Oasis Montaj Program Geosoft mapping and processing system: version 6.4.2 (HJ). Inc Suit 500, Richmond St. West Toronto, ON Canada N5S1V6, 2007.
7. Baranov V. 1957, A new method for interpretation of aeromagnetic maps: pseudo-gravimetric anomalies. *Geophysics*, vol. 22, no. 2, pp. 259–383. <https://doi.org/10.1190/1.1438369>
8. Baranov V., Naudy H. 1964, Numerical calculation of the formula of reduction to the magnetic pole. *Geophysics*, vol., no. 29, pp. 67–79. <https://doi.org/10.1190/1.1439334>
9. Baranov V. 1975, Potential fields and their transformation in applied geophysics. *Geo-exploration Monographs*, no. 6. Gebruder, Borntraeger. Berlin–Stuttgart, Series 1–6.
10. Bhattacharyya B. K. 1967, Some general properties of potential field in space and frequency domains. *Geoexploration*, vol. 5(3), pp. 127–143. [https://doi.org/10.1016/0016-7142\(67\)90021-X](https://doi.org/10.1016/0016-7142(67)90021-X)
11. Bhattacharyya B. K. 1965, Two-dimensional harmonic analysis as a tool for magnetic interpretation. *Geophysics*, vol. 30, no. 5, pp. 829–857. <https://doi.org/10.1190/1.1439658>
12. El-Hussaini A., Henain E. F. 1975, On the computation of second derivative from gravity data. Presented in the 9th Arab Petroleum Congress, Dubai.
13. Elkins T. A. 1951, The second derivative method of gravity interpretation. *Geophysics*, vol. 16, issue 1, pp. 29–50. <https://doi.org/10.1190/1.1437648>
14. Evjan H. M. 1936, The place of the vertical gradient in gravitational interpretation. *Geophysics*, vol. 1, issue 1, pp. 127–136. <https://doi.org/10.1190/1.1437067>
15. Henderson R. G. 1960, A comprehensive system of automatic computer in magnetic and gravity interpretation. *Geophysics*, vol. 25, issue 3, pp. 569–585. <https://doi.org/10.1190/1.1438736>

16. Henderson R. G., Zieltz L. 1949, The computation of second vertical derivative of geomagnetic fields. *Geophysics*, vol. 14, issue 4, pp. 517–534. <https://doi.org/10.1190/1.1437558>
17. Rosenbach O. 1953, A contribution to the computation of second derivative from gravity data. *Geophysics*, vol. 18, issue 4, pp. 894–912. <https://doi.org/10.1190/1.1437943>
18. Blakely R. J., Simpson R. W. 1986, Approximating edges of source bodies from magnetic or gravity anomalies. *Geophysics*, vol. 51, issue 7, pp. 1494–1498. <https://doi.org/10.1190/1.1442197>
19. Reid A. B., Allsop J. M., Granser H., Millett A. J., Somerton I. W. 1990, Magnetic interpretation in three dimensions using Euler deconvolution. *Geophysics*, vol. 55, issue 1, pp. 80–91. <https://doi.org/10.1190/1.1442774>
20. Klingele E. E., Marson L., Kahle H. G. 1991, Automatic interpretation of gravity gradiometric data in two dimensions: vertical gradient. *Geophysical Prospecting*, vol. 39, no. 3, pp. 407–434. <https://doi.org/10.1111/j.1365-2478.1991.tb00319.x>
21. Harris E., Jessell W., Barr T. 1996, Analysis of the Euler deconvolution techniques for calculating regional depth to basement in area of complex structures. SEG Annual Meeting, 10–15 November, Denver, Colorado.
22. Marson L., Klingele E. E. 1993, Advantage of using the vertical gradient of gravity for 3-D interpretation. *Geophysics*, vol. 58, issue 11, pp. 349–355. <https://doi.org/10.1190/1.1443374>
23. Stavrev P. Y. 1997, Euler deconvolution using differential similarity transforms of gravity or magnetic anomalies. *Geophysical Prospecting*, vol. 45, issue 2, pp. 207–246. <https://doi.org/10.1046/j.1365-2478.1997.00331.x>
24. Barbosa V., Sliva J., Medeiros W. 1999, Stability analysis and improvement of structural index in Euler deconvolution. *Geophysics*, vol. 64, issue 1, pp. 48–60. <https://doi.org/10.1190/1.1444529>
25. GMSYS Programs Gravity and Magnetic modeling, version 6.4.2 (HJ). Inc Suit 500, Richmond St. West Toronto, ON Canada N5S1V6, 2007.
26. GMSYS-3D Programs Gravity and Magnetic modeling, version 6.4.2 (HJ). Inc Suit 500, Richmond St. West Toronto, ON Canada N5S1V6, 2007.

The article was received on March 2, 2019

Интерпретация данных магниторазведки для определения глубины пород кристаллического фундамента и структурных элементов района Мандиша, оазис Эль-Бахария (Западная пустыня, Египет)

Вазль Рагаб ГАВЕИШ^{1, 2, *},
Хоссам Хассан МАРЗУК²,
Алексей Владимирович ПЕТРОВ¹,
Игорь Алексеевич МАРАЕВ¹

¹Российский государственный геологоразведочный университет, Россия, Москва

²Национальный научно-исследовательский институт астрономии и геофизики, Египет, Каир

Актуальность. Район исследования расположен в деревне Мандиша, оазис Эль-Бахария, Западная пустыня, Египет. Он страдает от недостатка поверхностных вод. Поэтому важно отыскать другой источник воды (например, грунтовые воды), необходимый для жизнедеятельности всего живого. На основании информации из литературы основной водоносный горизонт на исследуемой территории находится в Нубийском песчаном водоносном горизонте, который расположен непосредственно на верхней поверхности пород кристаллического фундамента. Таким образом, в районе исследований глубина нижней поверхности водоносного горизонта нубийского песчаника равна глубине верхней поверхности пород кристаллического фундамента.

Задачи исследования. В данной работе используются анализ и интерпретация данных магниторазведки для определения глубины пород кристаллического фундамента и структурных элементов, которые воздействовали на породы фундамента в районе Мандиша оазиса Эль-Бахария, Западная пустыня, Египет.

Методология исследования. Для выполнения поставленных задач были применены магнитные методы. Собраны данные со ста семидесяти четырех магнитных станций при помощи магнитометрического прибора Overhauser (GSM-19 «V7.0»). Данные магниторазведки были обработаны с использованием программы Geosoft Oasis Montaj. Показаны 2D магниторазведочный профиль и 3D моделирование магниторазведочных задач для построения рельефной карты фундамента в районе исследования. Деривативный метод, метод определения границ источника, 3D метод деконволюции Эйлера были применены с целью определения местоположений и направлений разломов, которые повлияли на породы кристаллического фундамента в области исследования.

Результаты работы. Наиболее важные результаты этого исследования: 1. Глубина пород кристаллического фундамента в районе исследования колеблется от 1200 до 2000 м. 2. Северо-восточная, северо-западная и западная части района исследований характеризуются малой глубиной пород фундамента, а южная и восточная части района исследований – большей глубиной. 3. Глубокие разломы (более 2000 м) были обнаружены в северной части района исследований. 4. Основными направлениями разломов в районе исследования являются северо-западное и восточное.

Ключевые слова: интерпретация данных магниторазведки, 3D метод деконволюции Эйлера, 2D магниторазведочный профиль, 3D моделирование магниторазведочных задач, порода кристаллического фундамента, разломы, Geosoft, оазис Эль-Бахария, Западная пустыня, Египет.

Статья поступила в редакцию 2 марта 2019 г.

* ✉ wael_ragab2007@yahoo.com

🆔 <http://orcid.org/0000-0002-5971-4839>